IOSR Journal of Electrical and Electronics Engineering (IOSR-JEEE)
e-ISSN: 2278-1676, p-ISSN: 2320-3331, Volume 19, Issue 1 Ser. 1 (Jan. – Feb. 2024), PP 15-27
www.iosrjournals.org

Propagation Along The Straight Waveguide With A Periodic Array In The Cross Section And The Behavior Of The Output Fields

Zion Menachem
Department Of Electrical Engineering, Sami Shamoon College Of Engineering, Israel

Abstract
The first objective in this research is to solve a wave propagation in a straight waveguide where the rectangular cross section consists of a periodic array with seven alternating hollow and dielectric layers. The analytical methods are not effective for solving complex inhomogeneous problems in the cross section of the waveguide. Therefore, it is necessary to find an effective numerical technique. We will develop an efficient technique that will solve this problem by using the mode model that based on Laplace and Fourier transforms and the inverse Laplace and Fourier transforms. The technique is important in order to generalize the mode model also for solve a complex and inhomogeneous problem in the cross section. The second and the main objective is to examine the effect of the wave propagation along a periodic array on the behaviorof the output fields. The application is effective in the microwave and millimeter-wave regimes.
Keywords: *Wave propagation, dielectric profiles, rectangular waveguide, dielectric material, rectangular cross section.*

Date of Submission: 01-01-2024 Date of acceptance: 11-01-2024

I. Introduction

The analytical methods are limited to relatively simple problems and over the years numerical methods and other interesting methods were proposed for solving complex problems. We will review examples of published articles that are based on interesting methods and techniques for a more efficient solution to complex problems in the cross section. Theoretical studies on microwave dielectric waveguides were presented in the previous publications using approximate or numerical methods. Two most common approximate techniques are the Marcatily approach [1] and the circular harmonic point matching technique [2]. Other approximate techniques were given in [3,4], by using the extended boundary condition method [3], and by using the rectangular harmonics [4].

A method of solving the propagation constant for the bound modes in the dielectric rectangular waveguides was introduced in [5]. This method provides a graphical solution of the characteristic equations obtained by complete mode matching at the interfaces of the guide without using any approximations. The rectangular dielectric waveguide technique was described in [6] for the determination of complex permittivity of a wide class of dielectric materials of various thicknesses and cross sections. This paper presents a unified rectangular dielectric waveguide technique for determination. A design strategy was proposed in [7] for microwave devices built with dielectric-loaded waveguides having one- or two-dimensional discontinuity profiles. The problem was formulated as an inverse problem where the predefined scattering parameters were aimed to be the final response of the system. This goal was achieved by optimizing the dimensions of the filling materials. To increase the success of the optimization, the problem was reduced to the longitudinal and widthwise thickness determination of the unit cell, which constitutes the whole structure in a cascade form. To this aim, the frequency response of the unit cell was targeted and then that of the whole system, which was achieved by a two-level optimization procedure of the unit cell.

A fundamental and accurate approach to compute the attenuation of electromagnetic waves propagating in dielectric rectangular waveguides were presented in [8]. The transverse wave numbers were first obtained as roots of a set of transcendental equations developed by matching fields with the fields with the surface impedance of the wall. The propagation constant was found by substituting the values of transverse wave numbers into the dispersion relation. The analysis also shows that a hollow waveguide was found to have much lower attenuation than its dielectric coun-teparts. Sinch the cutoff frequency is usually affected by the constitutive properties of the dielectric medium, for a waveguide designed for wave with the same cutoff frequency, hollow waveguides turn out to be relatively larger in size.

The radiation characteristics of an antenna composed by a rectangular guide loaded with dielectric

slab were analyzed and presented in [9]. A parametric study involving the dielectric loading level and the behavior of the cross-polarization was also included. The problem of electromagnetic-wave propagation in junctions between two symmetrically, partially dielectric-filled waveguides was investigated in [10], and the solution was presented in the form of a two-port equivalent circuit. The equivalent circuit includes an ideal 1:1 transformer, which is connected to transmission lines with impedances equal to those of the two waveguides, in cascade with a T network. Elements of the T network and the results were presented in graphs for different dielectric constants, slab thicknesses, and operating frequencies.

A partially filled waveguide method was presented in [11] that enhances transmission quality and accuracy in electromagnetic material but leads to the excitation of higher-order modes. A mode-matching technique was developed to accommodate the resulting waveguide discontinuity and a Newton root search method was utilized to subsequently extract the electromagnetic properties of the test sample.

A novel method for analyzing electromagnetic wave propagation in dielectric waveguides with arbitrary profiles was proposed in [12]. The transfer matrix function relates the wave profile at the output to the input wave in the Laplace space and is applicable for inhomogeneous dielectric profiles with single or multiple maxima in the transverse plane. The method is particularly useful for analyzing dielectric waveguides in the microwave and millimeter-wave regimes. This method is applicable for arbitrary profiles of the input field and the dielectric and is particularly useful for smoothly varying profiles. This makes it a versatile tool for analyzing a wide range of dielectric waveguides. The method is based on the Laplace and Fourier transforms, and the inverse Laplace and Fourier transforms.

In this research the first objective is to solve a propagation problem in a straight waveguide where the rectangular cross section consists of a periodic array with seven alternating hollow and dielectric layers, as shown in Fig.1. We will present an efficient technique to solve the inhomogeneous cross section of a periodic array with seven alternating hollow and dielectric layers. The technique is important in order to generalize the mode model [12] also to solve a complex and inhomogeneous problem in the cross section. The method is based on Laplace and Fourier transforms and the inverse Laplace and Fourier transforms. A Laplace transform is necessary to obtain convenient and simple input-output connections of the fields. The method is based on both the Fourier transform application and the wave equation solutions in a frequency domain. This paper is organized as follows. The periodic structure of the cross section of a rectangular waveguide is given in the second section. The proposed technique to solve a periodic array with seven alternating hollowand dielectric layers is given in the third section. The numerical results are presented in the fourth section, and conclusions are given in the last section.

II. The periodic structure of the cross section of a rectangular waveguide.

Figure 1 shows a rectangular cross section of a straight waveguide that consists of seven layers where the three layers 2, 4, and 6 are coated with a dielectric material.

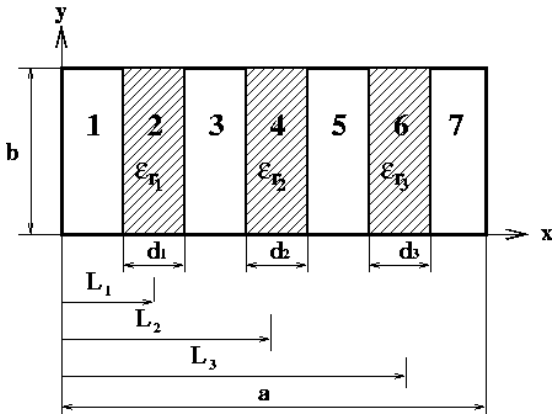

Figure 1: The cross section consists of a periodic array with seven alternating hollow and dielectric layers.

The dimensions of the cross section of the rectangular waveguide are denoted by the parameters a and b, where $0 \le x \le a$, and $0 \le y \le b$. This is an interesting structure of a periodic array that changes alternately between a hollow layer and a layer that is coated with a dielectric material. The parameters d_1, d_2 and d_3 are the thicknesses of the dielectric layers 2, 4, and 6, respectively. We assume that $d_1=d_2=d_3=d$. In addition, we assume that the dielectric material (ϵ_{r1}, ϵ_{r2}, ϵ_{r3}) in layers 2, 4, and 6 can be different. The parameters L_1, L_2, and L_3 are the distances from the left edge of the cross section to the middle of each thickness of the dielectric material, respectively.

III. The proposed technique to solve a periodic array with seven alternating hollow and dielectric layers by using the ω_ε function.

In order to solve a periodic array with seven alternating hollow and dielectric hollow and dielectric layers in the cross section (Fig. 1), we need to develop an exact expressions for the element of the matrices. In order to find the elements of the matrices of the inhomogeneous geometry of the cross section in Fig. 1, we can use with the ω_ε function [13]. Fig. 2 shows the ω_ε function. We need to take the limit $\varepsilon \longrightarrow 0$ for the ω_ε function, as shown in Fig. 2. The ω_ε function is defined as

$$\omega_\varepsilon(r) = C_\varepsilon \exp\left[-\frac{\varepsilon^2}{(\varepsilon^2 - |r|^2)}\right]. \qquad (1)$$

for $|r| > \varepsilon$, where C_ε is a constant, and $\int \omega_\varepsilon(r)dr = 1$. The ω_ε function enables us to solve an inhomogenous and discontinuous transition problem at the boundary between any hollow layer and a layer with a dielectric coating. In our cross section (Fig. 1), we have six discontinuous transitions. In each of the six transitions, we must use this ω_ε function.

for $|r| > \varepsilon$, where C_ε is a constant, and $\int \omega_\varepsilon(r)dr = 1$. The ω_ε function enables us to solve an inhomogenous and discontinuous transition problem at the boundary between any hollow layer and a layer with a dielectric coating. In our cross section (Fig. 1), we have six discontinuous transitions. In each of the six transitions, we must use this ω_ε function.

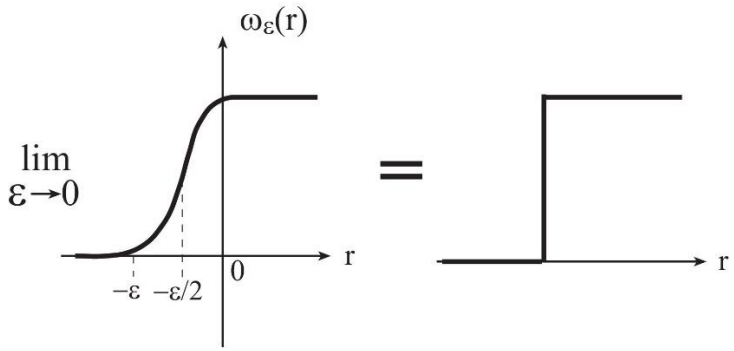

Figure 2: The ω_ε function (Eq. 1) for inhomogeneous problem of Fig. 1.

Figure 1 shows the cross section of the rectangular waveguide where the centers of the first, the second and the third dielectric rectangles relative to the X-axis are located at L_1=0.25 a, L_2=0.5 a, and L_3=0.75 a, respectively. The dimensions of the cross section of the rectangular waveguide are denoted by the parameters a and b, where $0 \le x \le a$, and $0 \le y \le b$. The parameters d_1, d_2 and d_3 are the thicknesses of the dielectric layers 2, 4, and 6, respectively. The elements of the matrix for these parameters are calculated according to

$$g(x)=\begin{cases} g_{01}\exp\left(1-q_1(x)\right) & \frac{\left(\frac{a}{2}\right)-d_1-\varepsilon}{2}\le x<\frac{\left(\frac{a}{2}\right)-d_1+\varepsilon}{2} \\ g_{01} & \frac{\left(\frac{a}{2}\right)-d_1+\varepsilon}{2}<x<\frac{\left(\frac{a}{2}\right)+d_1-\varepsilon}{2} \\ g_{01}\exp\left(1-q_2(x)\right) & \frac{\left(\frac{a}{2}\right)+d_1-\varepsilon}{2}\le x<\frac{\left(\frac{a}{2}\right)+d_1+\varepsilon}{2} \\ g_{02}\exp\left(1-q_3(x)\right) & \frac{(a)-d_2-\varepsilon}{2}\le x<\frac{(a)-d_2+\varepsilon}{2} \\ g_{02} & \frac{(a)-d_2+\varepsilon}{2}<x<\frac{(a)+d_2-\varepsilon}{2} \\ g_{02}\exp\left(1-q_4(x)\right) & \frac{(a)+d_2-\varepsilon}{2}\le x<\frac{(a)+d_2+\varepsilon}{2} \\ g_{03}\exp\left(1-q_5(x)\right) & \frac{\left(\frac{3a}{2}\right)-d_3-\varepsilon}{2}\le x<\frac{\left(\frac{3a}{2}\right)-d_3+\varepsilon}{2} \\ g_{03} & \frac{\left(\frac{3a}{2}\right)-d_3+\varepsilon}{2}<x<\frac{\left(\frac{3a}{2}\right)+d_3-\varepsilon}{2} \\ g_{03}\exp\left(1-q_6(x)\right) & \frac{\left(\frac{3a}{2}\right)+d_3-\varepsilon}{2}\le x<\frac{\left(\frac{3a}{2}\right)+d_3+\varepsilon}{2} \\ 0 & else \end{cases}$$

where $\varepsilon = a/50$, and where

$$q_1(x)=\frac{\varepsilon^2}{\varepsilon^2-[x-((a/2)-d_1+\varepsilon)/2]^2} \quad , \quad q_2(x)=\frac{\varepsilon^2}{\varepsilon^2-[x-((a/2)+d_1-\varepsilon)/2]^2},$$

$$q_3(x)=\frac{\varepsilon^2}{\varepsilon^2-[x-((a)-d_2+\varepsilon)/2]^2} \quad , \quad q_4(x)=\frac{\varepsilon^2}{\varepsilon^2-[x-((a)+d_2-\varepsilon)/2]^2}$$

$$q_5(x)=\frac{\varepsilon^2}{\varepsilon^2-[x-((3a/2)-d_3+\varepsilon)/2]^2} \quad , \quad q_6(x)=\frac{\varepsilon^2}{\varepsilon^2-[x-((3a/2)+d_3-\varepsilon)/2]^2}.$$

According to the image method, in order to force the boundary conditions at location of the walls in real problem, we need to extend the waveguide region of Fig. 1 ($0\le x\le a$, and $0\le y\le b$), to a four fold larger regions ($-a\le x\le a$, and $-b\le y\le b$). The boundary conditions and extend the problem to a periodic domain enable us the use of Fourier transform. By using with the image method and the ω_ε function, the elements of the matrix for the cross section of Fig. 1 are calculated in Fourier space by

$$g(n,m)=\frac{1}{ab}\{g_{01}\int_{((a/2)-d_1-\varepsilon)/2}^{((a/2)-d_1+\varepsilon)/2}\exp(1-q_1(x))\cos(\frac{n\pi x}{a})dx+$$

$$g_{01}\int_{((a/2)-d_1+\varepsilon)/2}^{((a/2)+d_1-\varepsilon)/2}\cos(\frac{n\pi x}{a})dx+g_{01}\int_{((a/2)+d_1-\varepsilon)/2}^{((a/2)+d_1+\varepsilon)/2}\exp(1-q_2(x))\cos(\frac{n\pi x}{a})dx+$$

$$g_{02}\int_{((a)-d_2-\varepsilon)/2}^{((a)-d_2+\varepsilon)/2}\exp(1-q_3(x))\cos(\frac{n\pi x}{a})dx+$$

$$g_{02}\int_{((a)-d_2+\varepsilon)/2}^{((a)+d_2-\varepsilon)/2}\cos(\frac{n\pi x}{a})dx+g_{02}\int_{((a)+d_2-\varepsilon)/2}^{((a)+d_2+\varepsilon)/2}\exp(1-q_4(x))\cos(\frac{n\pi x}{a})dx+$$

$$g_{03}\int_{((3a/2)-d_3-\varepsilon)/2}^{((3a/2)-d_3+\varepsilon)/2}\exp(1-q_5(x))\cos(\frac{n\pi x}{a})dx+$$

$$g_{03}\int_{((3a/2)-d_3+\varepsilon)/2}^{((3a/2)+d_3-\varepsilon)/2}\cos(\frac{n\pi x}{a})dx + g_{03}\int_{((3a/2)+d_3-\varepsilon)/2}^{((3a/2)+d_3+\varepsilon)/2}\exp(1-q_6(x))\cos(\frac{n\pi x}{a})dx\}$$

$$\left\{\int_0^b \cos\left(\frac{m\pi y}{b}\right)dy\right\}. \qquad (2)$$

From the elements of the matrix we obtain the matrix G given in Appendix A. It is important to note that this is a special matrix. Similarly, the G_x matrix is obtained by the derivative of the Fourier components of the dielectric profile. The derivative of the dielectric profile (g_x) is defined as

$$g_x \equiv \frac{1}{\epsilon(x,y)}\frac{\partial\epsilon(x,y)}{\partial x} = \frac{\partial\left[\ln\left(1+g(x,y)\right)\right]}{\partial x}. \qquad (3)$$

Therfore, according to Eq. (3) and the cross section of Fig. 1, we obtain

$$g_x(x) = \begin{cases} \frac{d}{dx}\left[\ln\left(1+g_{01}\exp\left(1-q_1(x)\right)\right)\right] & \frac{\left(\frac{a}{2}\right)-d_1-\varepsilon}{2} \le x < \frac{\left(\frac{a}{2}\right)-d_1+\varepsilon}{2} \\ 0 & \frac{\left(\frac{a}{2}\right)-d_1+\varepsilon}{2} < x < \frac{\left(\frac{a}{2}\right)+d_1-\varepsilon}{2} \\ \frac{d}{dx}\left[\ln\left(1+g_{01}\exp\left(1-q_2(x)\right)\right)\right] & \frac{\left(\frac{a}{2}\right)+d_1-\varepsilon}{2} \le x < \frac{\left(\frac{a}{2}\right)+d_1+\varepsilon}{2} \\ \frac{d}{dx}\left[\ln\left(1+g_{02}\exp\left(1-q_3(x)\right)\right)\right] & \frac{(a)-d_2-\varepsilon}{2} \le x < \frac{(a)-d_2+\varepsilon}{2} \\ 0 & \frac{(a)-d_2+\varepsilon}{2} < x < \frac{(a)+d_2-\varepsilon}{2} \\ \frac{d}{dx}\left[\ln\left(1+g_{02}\exp\left(1-q_4(x)\right)\right)\right] & \frac{(a)+d_2-\varepsilon}{2} \le x < \frac{(a)+d_2+\varepsilon}{2} \\ \frac{d}{dx}\left[\ln\left(1+g_{03}\exp\left(1-q_5(x)\right)\right)\right] & \frac{\left(\frac{3a}{2}\right)-d_3-\varepsilon}{2} \le x < \frac{\left(\frac{3a}{2}\right)-d_3+\varepsilon}{2} \\ 0 & \frac{\left(\frac{3a}{2}\right)-d_3+\varepsilon}{2} < x < \frac{\left(\frac{3a}{2}\right)+d_3-\varepsilon}{2} \\ \frac{d}{dx}\left[\ln\left(1+g_{03}\exp\left(1-q_6(x)\right)\right)\right] & \frac{\left(\frac{3a}{2}\right)+d_3-\varepsilon}{2} \le x < \frac{\left(\frac{3a}{2}\right)+d_3+\varepsilon}{2} \\ 0 & else \end{cases}. \qquad (4)$$

The elements of the matrix for the derivative of the dielectric profile is given by

$$g_x(n,0) = \frac{1}{a}\{\lim_{\epsilon\to\infty}\int_{((a/2)-d_1-\varepsilon)/2}^{((a/2)-d_1+\varepsilon)/2}\cos(\frac{n\pi x}{a})\frac{d}{dx}[\ln(1+g_{01}\exp(1-q_1(x)))]dx +$$

$$\lim_{\epsilon\to\infty}\int_{((a/2)+d_1-\varepsilon)/2}^{((a/2)+d_1+\varepsilon)/2}\cos(\frac{n\pi x}{a})\frac{d}{dx}[\ln(1+g_{01}\exp(1-q_2(x)))]dx +$$

$$\lim_{\epsilon\to\infty}\int_{((a)-d_2-\varepsilon)/2}^{((a)-d_2+\varepsilon)/2}\cos(\frac{n\pi x}{a})\frac{d}{dx}[\ln(1+g_{02}\exp(1-q_3(x)))]dx +$$

$$\lim_{\epsilon\to\infty}\int_{((a)+d_2-\varepsilon)/2}^{((a)+d_2+\varepsilon)/2}\cos(\frac{n\pi x}{a})\frac{d}{dx}[\ln(1+g_{02}\exp(1-q_4(x)))]dx +$$

$$\lim_{\epsilon\to\infty}\int_{((3a/2)-d_3-\varepsilon)/2}^{((3a/2)-d_3+\varepsilon)/2}\cos(\frac{n\pi x}{a})\frac{d}{dx}[\ln(1+g_{03}\exp(1-q_5(x)))]dx +$$

$$\lim_{\epsilon\to\infty}\int_{\frac{\left(\frac{3a}{2}\right)+d_3-\varepsilon}{2}}^{\frac{\left(\frac{3a}{2}\right)+d_3+\varepsilon}{2}}\cos(\frac{n\pi x}{a})\frac{d}{dx}[\ln(1+g_{03}\exp(1-q_6(x)))]dx\}. \qquad (5)$$

The matrix of the dielectric profile is given in Appendix A. We see that this is a special matrix. The

components of the fields obtained at the output of the straight waveguide according to the mode model [12] are briefly given in Appendix B. From the development of the matrices for the complex and inhomogeneous cross section (Fig. 1), we can use the components of the output fields as given in Appendix B and we also need to use Laplace and Fourier transforms on the components of the output fields.

IV. Numerical results

This section presents several examples for the propagation along a rectangular cross section as shown in Fig. 1. The cross section consists of a periodic array with seven alternating hollow and dielectric layers. All the next graphical results are demonstrated as a response to a half-sine (TE_{10}) input- wave profile and the inhomogeneous geometries of the cross section. All the results are demonstrated for a=b=20 *mm,* $k_0 = 167$ *1/m*, $\lambda = 3.75$ *cm*, $\beta = 58$ *1/m,* and z= 0.15 *m*.

In this study, the parameters L_1=0.25 a, L_2=0.5 a, and L_3=0.75 a are the distances from the left edge of the cross section to the middle of each thickness of the dielectric material, respectively,as shown in Fig.1. The parameters d_1, d_2 and d_3 are the thicknesses of the dielectric layers 2, 4, and 6, respectively. We assume that d_1=d_2=d_3=d and that dielectric material (ϵ_{r1}, ϵ_{r2}, ϵ_{r3}) in layers 2, 4, and 6 can be different.

Figures 3(a)-3(e) show the output field for the propagation along a rectangular cross section, where a=b=20 *mm,* d=a/7=2.86 *mm*, for $\epsilon_{r1} = \epsilon_{r2} = \epsilon_{r3} = 7$ (Fig. 3a), $\epsilon_{r1} = \epsilon_{r2} = \epsilon_{r3} = 8$ (Fig. 3b), $\epsilon_{r1} = \epsilon_{r2} = \epsilon_{r3} = 9$ (Fig. 3c), and $\epsilon_{r1} = \epsilon_{r2} = \epsilon_{r3} = 10$ (Fig. 3d). Fig. 3(e) shows the output field for the same cross section of the results Figs.3(a)-3(d) where $\epsilon_{r1} = \epsilon_{r2} = \epsilon_{r3} = \epsilon_r = 7$, 8, 9,and 10, respectively, and for x-axis where y=b/2=10 mm.

Figures 4(a)-4(e) show the output field for the propagation along a rectangular cross section where a=b=20 *mm* and d=a/7=2.86 *mm*. This case is demonstrated for $\epsilon_{r1} = \epsilon_{r3} = 1$, where $\epsilon_{r2} = 7$ (Fig. 4a), $\epsilon_{r2} = 8$ (Fig. 4b), $\epsilon_{r2} = 9$ (Fig. 4c), and $\epsilon_{r2} = 10$ (Fig. 4d). Fig. 4(e) shows the output field for the same cross section of the results Figs.(4a) - (4d) where $\epsilon_{r2} = \epsilon_r = 7$, 8, 9, and 10, respectively, and for x-axis where y=b/2=10 mm.

Figures 4(a)-4(e) show an interesting case in relation to Figs. 3(a)-3(e). In this case the dielectric layer is located at the middle of the cross section and the results of Figs. 4(a)-(e) are logical. The half-sine profile is dominant for the dielectric profile for each value of ϵ_r.

Figures 5(a)-5(e) show the output field in relation to Figs. 3(a)-(e), by only decreasing the thickness of each dielectric layer from d=a/7=2.86 *mm* to d=a/8=2.5 *mm*, where the other parameters are not changed. By only decreasing the thickness of each of the three layers coated with a dielectric material, the behavior of the output fields and the amplitudes are changed significantly. Figures 6(a)-6(e) show the output field in relation to Figs. 4(a)-(e), by only decreasing the thickness of each dielectric layer from d=a/7=2.86 *mm* to d=a/8=2.5 *mm*, where the other parameters are not changed.

From the results we see that by increasing ϵ_r, the amplitude of the output field decreases, and the width of the output profile is smaller.

From all the graphical results, the dominant parameters that influence on the behavior of the output fields are the dimensions of the cross section, the dielectric profile, the thickness of the dielectric layers and their locations.

V. Conclusions

The first objective in this research was to solve a wave propagation in a straight waveguide where the rectangular cross section consists of a periodic array with seven alternating hollow and dielectric layers. The second and the main objective in this study was to show the effect of propagation in a straight waveguide with this interesting cross-section on the behavior of the fields at the output of the waveguide. The application is effective in the millimeter regime. All the graphical results are demonstrated as a response to a half-sine (TE_{10}) input-wave profile and the inhomogeneous geometries of the cross section.

Figures 4(a)-4(e) show an interesting case in relation to Figs. 3(a)-3(e). In this case the dielectric layer is located at the middle of the cross section and the results of Figs. 4(a)-(e) are logical. The half-sine profile is dominant for the dielectric profile for each value of ϵ_r.

Figures 5(a)-5(e) show the output field in relation to Figs. 3(a)-(e), by only decreasing the thickness of each dielectric layer from d=a/7=2.86 *mm* to d=a/8=2.5 *mm*, where the other parameters are not changed. By only decreasing the thickness of each of the three layers coated with a dielectric material, the behavior of the output fields and the amplitudes are changed significantly.Figures 6(a)-6(e) show the output field in relation to Figs. 4(a)-(e), by only decreasing the thickness of each dielectric layer from d=a/7=2.86 *mm* to d=a/8=2.5 *mm*, where the other parameters are not changed.

From the results we see that by increasing ϵ_r, the amplitude of the output field decreases, and the

width of the output profile is smaller.

From all the graphical results, the dominant parameters that influence on the behavior of the output fields are the dimensions of the cross section, the dielectric profile, the thickness of the dielectric layers and their locations.

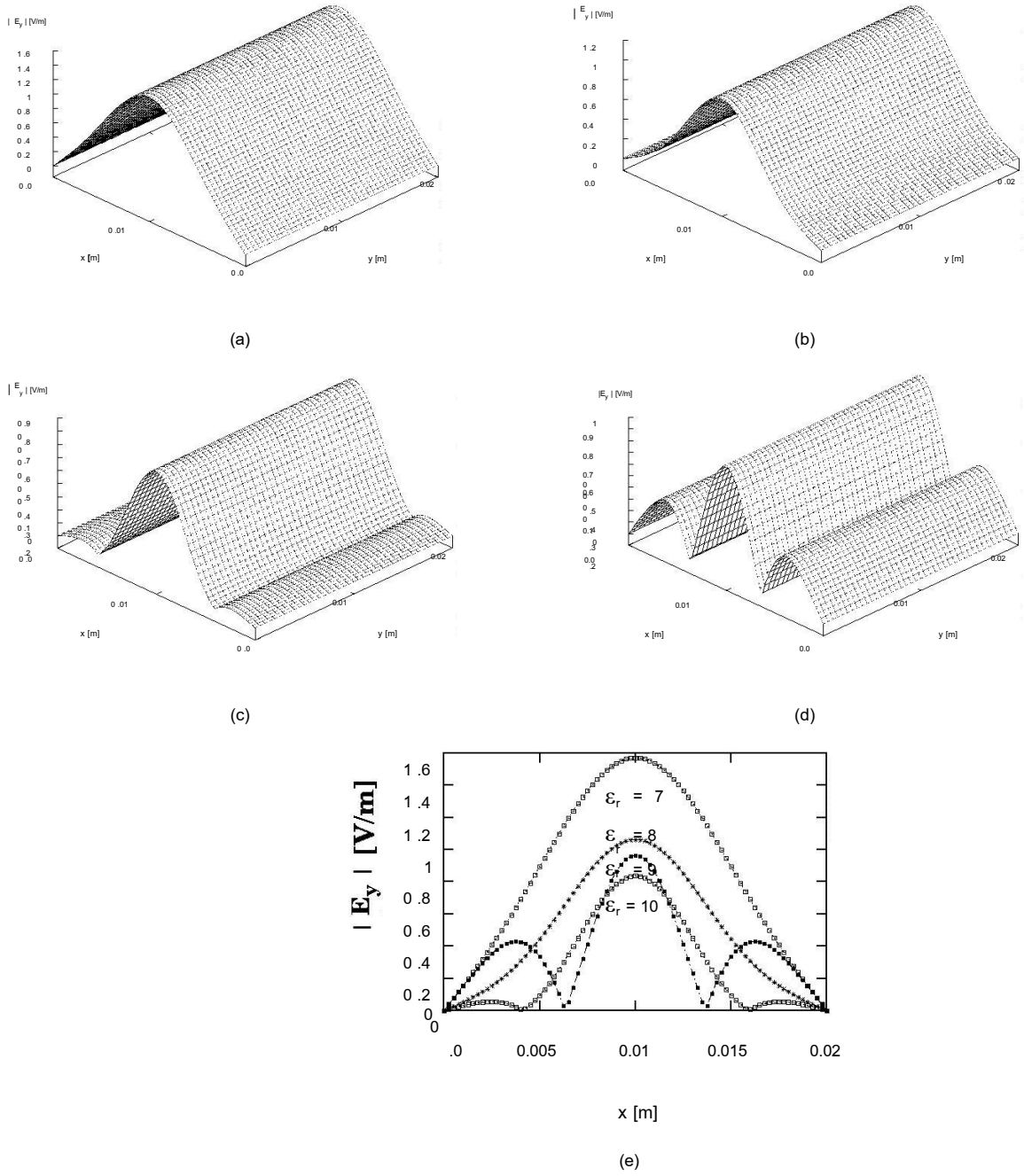

Figure 3: The output field for the propagation along a rectangular cross section (Fig.1), where a=b=20 mm, and d=a/7=2.86 mm. This case is demonstrated for (a) $\varepsilon_{r1} = \varepsilon_{r2} = \varepsilon_{r3} = 7$, (b) $\varepsilon_{r1} = \varepsilon_{r2} = \varepsilon_{r3} = 8$, (c) $\varepsilon_{r1} = \varepsilon_{r2} = \varepsilon_{r3} = 9$, and (d) $\varepsilon_{r1} = \varepsilon_{r2} = \varepsilon_{r3} = 10$. (e). The output field in the same cross section of the results (a)-(d) where $\varepsilon_{r1} = \varepsilon_{r2} = \varepsilon_{r3} = \varepsilon_r = 7$, 8, 9, and 10, respectively, for x-axis where y=b/2=10 mm.

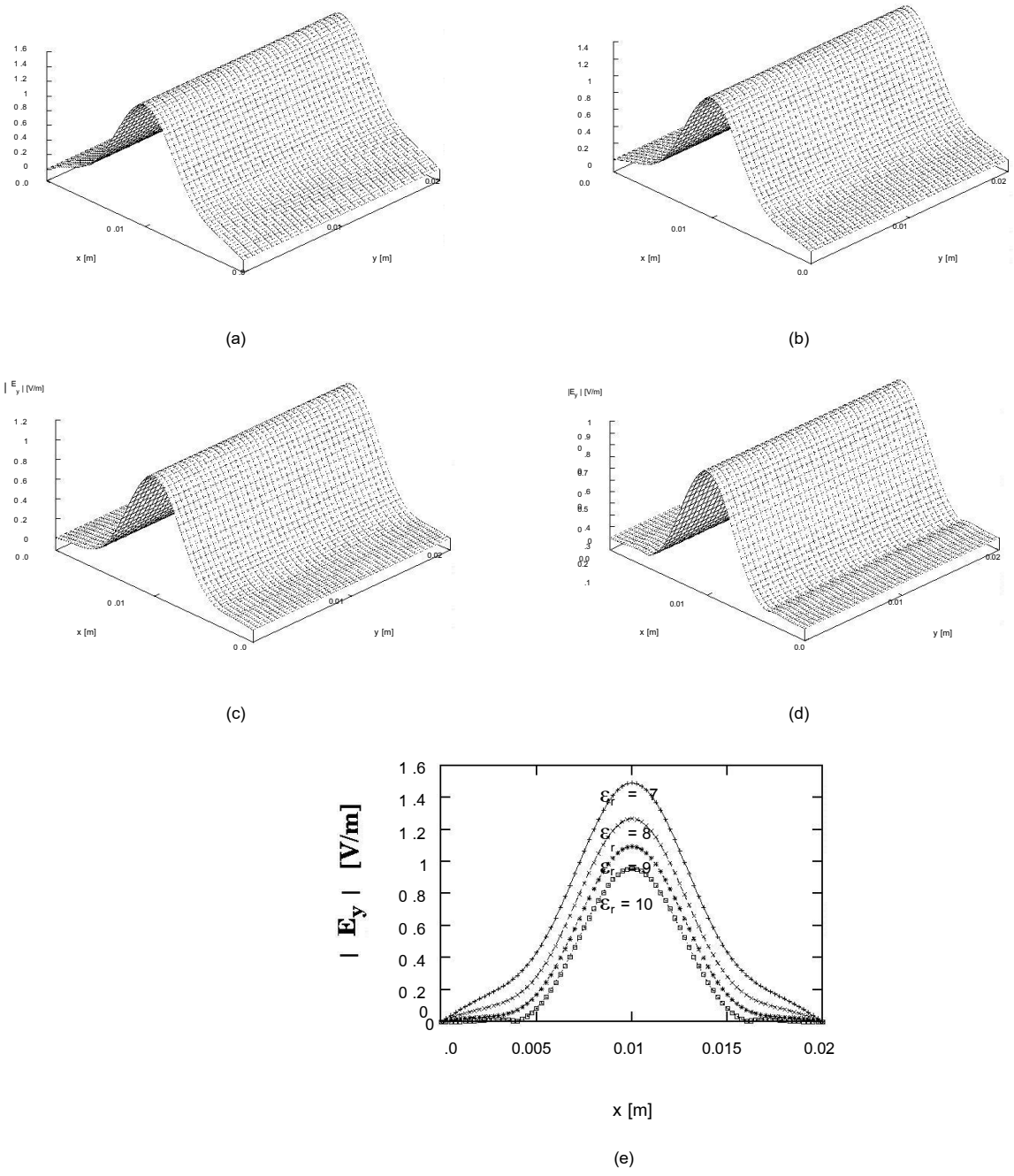

Figure 4: The output field for the propagation along a rectangular cross section (Fig.1), where a=b=20 mm, and d=a/7=2.86 mm. This case is demonstrated for $\varepsilon_{r1} = \varepsilon_{r3} = 1$, where (a) $\varepsilon_{r2} = 7$, (b) $\varepsilon_{r2} = 8$, (c) $\varepsilon_{r2} = 9$, and (d) $\varepsilon_{r2} = 10$. (e). The output field in the same cross section of the results (a)-(d) where $\varepsilon_{r2} = \varepsilon_{r} = 7, 8, 9,$ and 10, respectively, for x-axis where y=b/2=10 mm.

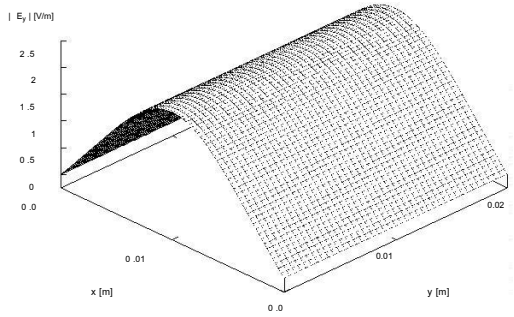

(a)

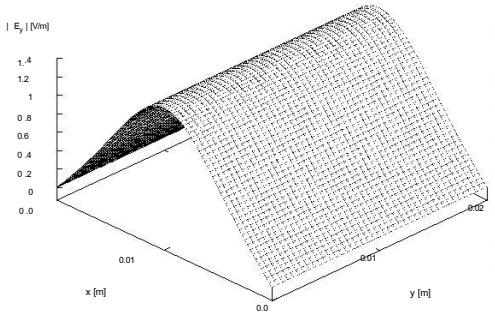

(b)

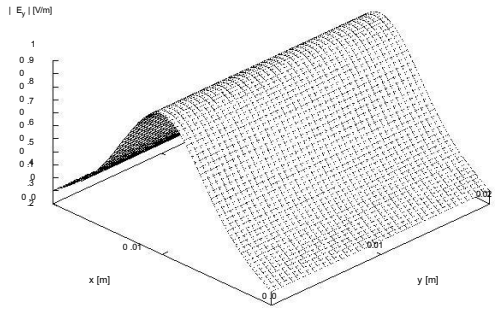

(c)

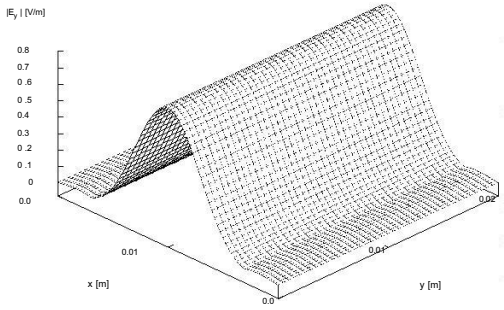

(d)

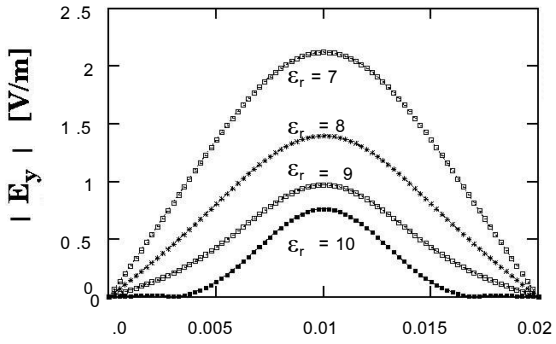

(e)

Figure 5: The output field for the propagation along a rectangular cross section (Fig.1), where a=b=20 mm, and d=a/8=2.5 mm. This case is demonstrated for (a) $\varepsilon_{r1} = \varepsilon_{r2} = \varepsilon_{r3} = 7$,

(b) $\varepsilon_{r1} = \varepsilon_{r2} = \varepsilon_{r3} = 8$, (c) $\varepsilon_{r1} = \varepsilon_{r2} = \varepsilon_{r3} = 9$, and (d) $\varepsilon_{r1} = \varepsilon_{r2} = \varepsilon_{r3} = 10$. (e). The output field in the same cross section of the results (a)-(d) where $\varepsilon_{r1} = \varepsilon_{r2} = \varepsilon_{r3} = \varepsilon_r = 7$, 8, 9, and 10, respectively, for x-axis where y=b/2=10 mm.

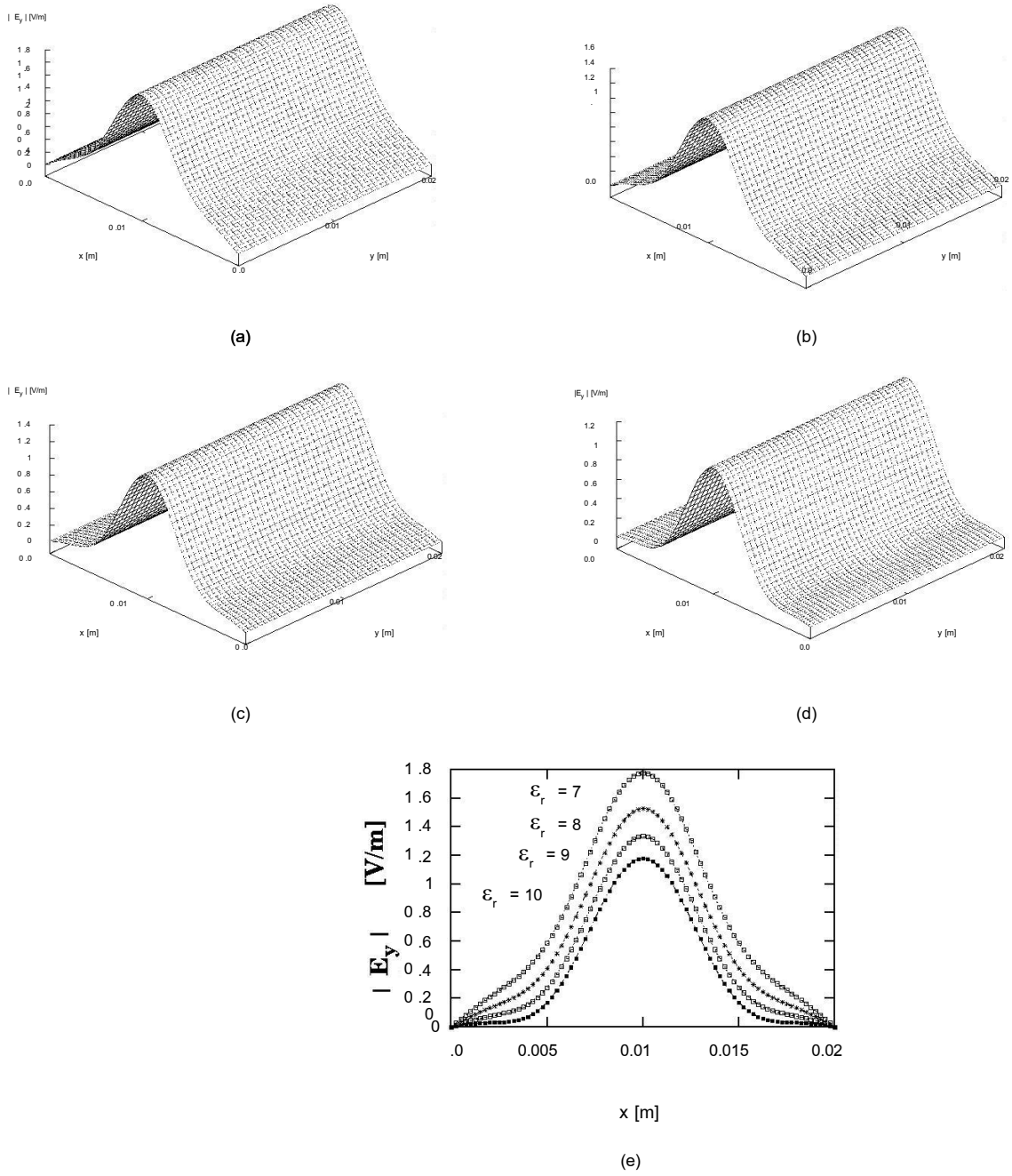

Figure 6: The output field for the propagation along a rectangular cross section (Fig.1), where a=b=20 mm, and d=a/8=2.5 mm. This case is demonstrated for $\varepsilon_{r1} = \varepsilon_{r3} = 1$, where (a) $\varepsilon_{r2} = 7$, (b) $\varepsilon_{r2} = 8$, (c) $\varepsilon_{r2} = 9$, and (d) $\varepsilon_{r2} = 10$. (e). The output field in the same cross section of the results (a)-(d) where $\varepsilon_{r2} = \varepsilon_r = 7$, 8, 9, and 10, respectively, for x-axis where y=b/2=10 mm.

Appendix A

The matrix G is given by the form

$$G = \begin{bmatrix} g_{00} & g_{-10} & g_{-20} & \cdots & g_{-nm} & \cdots & g_{-NM} \\ g_{10} & g_{00} & g_{-10} & \cdots & g_{-(n-1)m} & \cdots & g_{-(N-1)M} \\ g_{20} & g_{10} & \ddots & \ddots & \ddots & & \\ \vdots & g_{20} & \ddots & \ddots & \ddots & & \\ g_{nm} & \ddots & \ddots & \ddots & g_{00} & \vdots & \\ \vdots & & & & & & \\ g_{NM} & \cdots & \cdots & \cdots & \cdots & \cdots & g_{00} \end{bmatrix}$$

Appendix B

The output components of the electric field according to [12] are given by

$$E_x = \{D_x + \alpha_1 M_1 M_2\}^{-1}\left(\hat{E}_{x_0} - \alpha_2 M_1 \hat{E}_{y_0}\right), \qquad (A-2b)$$

$$E_y = \left\{D_y + \alpha_1 M_3 M_4\right\}^{-1}\left(\hat{E}_{y_0} - \alpha_3 M_3 \hat{E}_{x_0}\right), \qquad (A-2b)$$

$$E_z = {D_z}^{-1}\left\{\hat{E}_{z_0} + \frac{1}{2s}(G_x E_{x_0} + G_y E_{y_0}) - \frac{1}{2}(G_x E_x + G_y E_y)\right\}, \qquad (A-2c)$$

where $E_{x_0}, E_{y_0}, E_{z_0}$ are the initial values of the corresponding fields at z=0, i.e., $E_{x_0} = E_x$ (x, y, z=0), and $\hat{E}_{x_0}, \hat{E}_{y_0}, \hat{E}_{z_0}$ are the initial-value vectors,

$$D_x \equiv K^{(0)} + \frac{k_o^2 \chi_0}{2s} G + \frac{jk_{ox}}{2s} N G_x, \quad D_y \equiv K^{(0)} + \frac{k_o^2 \chi_0}{2s} G + \frac{jk_{oy}}{2s} M G_y, \quad D_z \equiv K^{(0)} + \frac{k_o^2 \chi_0}{2s} G,$$

$$K^{(0)}{}_{(n,m)(n\prime,m\prime)} = \{[k_o^2 - (n\pi/a)^2 - (m\pi/b)^2 + s^2]/2s\}\delta_{nn\prime}\delta_{mm\prime},$$

$$M_{(n,m)(n\prime,m\prime)} = m\delta_{nn\prime}\delta_{mm\prime}, \quad N_{(n,m)(n\prime,m\prime)} = n\delta_{nn\prime}\delta_{mm\prime},$$

$$\alpha_1 = \frac{k_{ox}k_{oy}}{4s^2}, \quad \alpha_2 = \frac{jk_{ox}}{2s}, \quad \alpha_3 = \frac{jk_{oy}}{2s},$$

$$M_1 = NG_y{D_y}^{-1}, \quad M_2 = MG_x, \quad M_3 = MG_x{D_x}^{-1}, \quad M_4 = NG_y.$$

References

[1] Marcatili, E. A. J.," Dielectric Rectangular Waveguide And Directional Couplers For Integrated Optics," Bell Syst. Tech. J., Vol.48, 2071, 1969.

[2] Goell, J. E.," A Circular-Harmonic Computer Analysis Of Rectangular Dielectric Waveguides," BellSyst. Tech. J., Vol.48, 2133, 1969.

[3] Eyges, L., P. Gianino, And P. Wintersteiner," Modes Of Dielectric Waveguides Of Arbitrary Cross Sectional Shapes," J. Opt. Soc. Am., Vol. 69, 1226, 1979.

[4] Schlosser, W. And H. G. Unger," Advances In Microwaves," Academic Press, New York, 1966.

[5] Jigyasa S., And Asok D.," Full-Wave Analysis Of Dielectric Rectangular Waveguides," Progress In Electromagnetics Research M, Vol. 13, 121-131, 2010.

[6] Zulkifly A., Roger D. P., And Robert W. K.," A Rectangular Dielectric Waveguide Technique For Determination Of Permittivity Of Materials At W-Band," IEEE Transactions On MicrowaveTheory And Techniques, Vol. 46, 2011-2015, 1999.

[7] Ahmet A., And Funda A.,," Synthesis Of Dielectric-Loaded Waveguide Filters As An Inverse Prob- Lem," Applied Mathematics In Science And Engineering, Vol. 30, 376-396, 2022.

[8] Kim H. Y., Kai H. T., Kee C. Y., Koon C. L., And Me C. L.," Propagation In Dielectric Rectangular Waveguides," Optica Applicata, Vol. XLVI, 317-330, 2016.

[9] Vital D. S., And Descardeci J. R.," Parametric Analysis Of Open-Ended Dielectric-Slab-Loaded Rectangular Waveguide," Journal Of Microwaves And Optoelectronics, Vol. 2, 22-29, 2001.

[10] Chang C. T. M.," Equivalent Circuit For Partial Dielectric-Filled Rectangular-Waveguide," Ieee Transactions On Microwave Theory And Techniques, Vol. 21, 403-411, 1973.

[11] Bogle A., Havrilla M., Nyquis D., Kemple L., And Rothwell E.," Electromagnetic Material Characterization Using A Partially-Filled Rectangular Waveguide," Journal Of Electromagnetic Waves And Applications, Vol. 19, 1291-1306,

2012.
[12] Menachem, Z., And E. Jerby," Transfer Matrix Function (TMF) For Propagation In Dielectric Waveguides With Arbitrary Transverse Profiles," IEEE Transactions On Microwave Theory AndTechniques, Vol. 46, 975-982, 1998.
[13] Vladimirov V.," Equations Of Mathematical Physics," New York, Marcel Dekker, Inc., 1971.